

Dimensional crossover and absence of quantum criticality in $\text{SrTi}^{16}\text{O}_{1-x}\text{}^{18}\text{O}_x$

A. Bussmann-Holder¹ and A. R. Bishop²

¹Max-Planck-Institute for Solid State Research, Heisenbergstrasse 1, D-70569 Stuttgart, Germany

²Los Alamos National Laboratory, Los Alamos, New Mexico 87545, USA

(Received 6 August 2008; published 26 September 2008)

The isotope-induced ferroelectricity observed in $\text{SrTi}^{18}\text{O}_3$ (STO18) enables a systematic study of the crossover between quantum paraelectricity and ferroelectricity as a function of x in $\text{SrTi}^{16}\text{O}_{1-x}\text{}^{18}\text{O}_x$ (STO16_{1-x}STO18_x). We predict that all ferroelectric compounds have a finite transition temperature T_c and show a dimensionality crossover from $d=3$ to $d=4$ at sufficiently low temperature. A discontinuity in behavior takes place around $x=0.35$, where quantum fluctuations suppress the transition. No evidence is found for a quantum critical point in the phase diagram. The high temperature structural transition shows a substantial isotope dependence which is, however, less striking than for the ferroelectric transition.

DOI: 10.1103/PhysRevB.78.104117

PACS number(s): 77.80.-e, 64.70.K-, 63.20.Ry

$\text{SrTi}^{16}\text{O}_3$ has been known for more than 50 years and is one of the best investigated perovskite oxides. Around $T_s = 105$ K a structural instability takes place which is accompanied by the freezing of a zone-boundary mode.^{1,2} Simultaneously, a long-wavelength optic mode decreases in energy and is reminiscent of a ferroelectric instability.³ An extrapolation of its frequency to zero suggests a ferroelectric phase-transition temperature of $T_c = 17$ K. This instability does not take place, however, since quantum fluctuations set in and dominate the low-temperature dynamical properties. In this regime, temperature is an inappropriate parameter for a phase diagram and the dielectric properties. As a consequence the system was termed a “quantum paraelectric.”⁴ An analogous behavior is observed in KTaO_3 (Ref. 5) and CaTiO_3 .⁶ In all these compounds ferroelectricity can be induced by sufficient doping. In $\text{SrTi}^{16}\text{O}_3$ (STO16) Ca doping leads to finite values of T_c , and an interesting crossover from a XY $n=2$ quantum ferroelectric to a random field-induced domain state takes place with increased Ca doping.⁷ Another route to inducing ferroelectricity in STO16 has recently been realized by replacing ^{16}O by its isotope ^{18}O .⁸ Here, the instability takes place at $T_c = 24$ K and both phases, the ferroelectric and the paraelectric ones, have subsequently been investigated in detail.⁹ While long-wavelength probes such as Raman scattering or infrared studies provide evidence for a purely displacive transition with perfect mode softening,^{10,11} local probes such as NMR or EPR support an order/disorder-driven phase transition.¹² That both dynamics can coexist has been shown theoretically, and this can resolve the apparent experimental controversy.¹³ The higher temperature structural phase transition has been the focus of detailed experimental investigations, since it was early suggested that also here order/disorder and displacive dynamics accompany this instability.^{14–16} In particular, a two component approach was developed, since a central peak emerges upon approaching T_s which increases in intensity with decreasing temperature.^{15,16} An explanation of this observation has been given in terms of intrinsic or quenched defects,^{17,18} intrinsic effects, and quasistatic domains,^{19,20} and recently been shown to be intrinsic.¹¹

In the following, we primarily concentrate on the x -dependent phase diagram of STO16_{1-x}STO18_x, which of-

fers a unique opportunity to investigate the crossover to quantum paraelectric behavior and dimensionality crossover within the same system, and where doping induced changes of the lattice potential and dynamics can be ruled out. The quantum limit of phase transitions has been intensively studied by various approaches. Oppermann and Thomas²¹ studied the critical behavior in the displacive limit for a Φ_4 model and predicted a change in the scaling relations in the quantum regime. Schneider *et al.*²² investigated this limit within a n -component vector model for structural phase transitions and observed that the leading exponent γ of the dielectric susceptibility changes from $\gamma=1$ to $\gamma=2$. A dimensionality crossover has been found by renormalization-group theory,²³ where quantum fluctuations enhance the system's effective dimension and give rise to new critical exponents, with the $\gamma=2$ quantum paraelectric limit exhibiting additional logarithmic corrections. Scaling properties in the quantum limit have been investigated for the case of quantum paraelectric solid solutions of $\text{SrTiO}_3:\text{Ca}$, where both the displacive and the order-disorder limit have been considered.²⁴ In the displacive limit the phenomenological Barrett formula²⁵ has been recovered which yields, however, a much poorer agreement with experimental data for STO16 (Ref. 4) than the analysis within the polarizability model.^{26,27} A very different examination of the quantum phase transition has been given by Rubtsov and Janssen,²⁸ who studied the discrete Φ_4 model in two dimension (2D) and three dimension (3D). They found that the transition can be changed continuously from soft mode to the transverse Ising behavior by varying the model parameters. Experimentally, the quantum regime has been studied in detail in $\text{KTa}_{1-x}\text{Nb}_x\text{O}_3$ and $\text{K}_{1-y}\text{Na}_y\text{TaO}_3$ and been interpreted within the polarizability model.²⁹ In these doped compounds the crossover from $\gamma=1$ (classical regime) to $\gamma=2$ (quantum regime) could be well established. More recently a variety of studies on doped perovskites have been performed concentrating on the quantum critical regime.^{30,31}

In addition to this low-temperature regime, we also investigate the isotope dependence of the structural instability. Since this is driven by the polarizability¹³ of the long-wavelength soft mode, an isotope effect is present here as well which is absent in conventional Φ_4 theories.

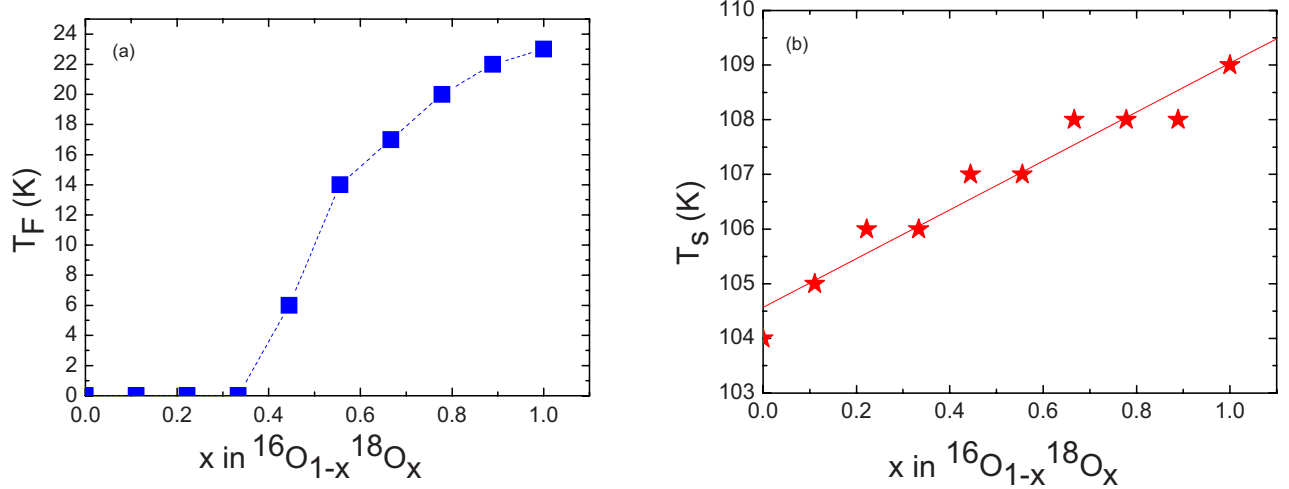


FIG. 1. (Color online) (a) x dependence of the ferroelectric phase-transition temperature T_c in $\text{STO}_{16_{1-x}}\text{STO}_{18_x}$. The squares for $x < 0.35$ do not refer to $T_c = 0$ K, but indicate that quantum fluctuations suppress the ferroelectric instability. (b) x dependence of the structural phase-transition temperature T_s in $\text{STO}_{16_{1-x}}\text{STO}_{18_x}$. The stars are results from the model calculation, the line is a guide to the eye.

Here, we use a polarizability model^{11,13,27,32} to study the phase diagram of $\text{STO}_{16_{1-x}}\text{STO}_{18_x}$, where nonlinear electron-ion interactions represent essential charge-transfer hybridizations of oxygen p and transition-metal d orbitals. These hybridizations experience a redistribution³² with decreasing temperature and trigger the phase transition. The model Hamiltonian is given by

$$H = \frac{1}{2} \sum_n \left[M_{1n} \dot{u}_{1n}^2 + m_2 \dot{u}_{2n}^2 + f'(u_{1n+1} - u_{1n})^2 + f(v_{1n} - u_{2n})^2 + f(v_{1n+1} - u_{2n})^2 + g_2 w_{1n}^2 + \frac{1}{2} g_4 w_{1n}^4 \right]. \quad (1)$$

The first two terms are the ionic core kinetic energies for ionic masses $M_1(\text{TiO}_3)$ and $m_2(\text{Sr})$ with site n dependent displacement coordinates u_{in} , $i=1,2$. The polarizability coordinate $w_{1n} = v_{1n} - u_{1n}$ is the relative displacement between the shell and core of the polarizable unit TiO_3 . f, f' are harmonic nearest- and second-nearest-neighbor coupling constants; g_2, g_4 define the local double-well potential in the polarizability, since $g_2 < 0, g_4 > 0$. The model parameters are the same as in Refs. 11 and 13 with the same oxygen ion mass renormalization as used in Refs. 11 and 13. The variation of $M_1(\text{TiO}_3)$ with x is simply linear as in our previous work and shown in Fig. 1. The nonlinear term is treated within the self-consistent phonon approximation (SPA) corresponding to a cumulant expansion in w , whereby an effectively harmonic but temperature dependent local coupling constant g_T is defined

$$g_T = g_2 + 3g_4 \langle w^2 \rangle_T, \quad \langle w^2 \rangle_T = \sum_{q,j} \frac{\hbar}{2N\omega_{q,j}} w_{1n}^2(q,j) \coth \frac{\hbar\omega_{q,j}}{2kT}. \quad (2)$$

In this approach, the dynamical information enters through the branch j and momentum q dependent eigenvalues. For the numerical calculation the summation in Eq. (2) is replaced by its integral where a three-dimensional integration

in momentum space is carried through guaranteeing that an instability takes place. The three-dimensional integration approximates the phonon mode dispersion by an isotropic one. That this treatment is equivalent to the full 3D calculation has been established in a variety of work where quantitative agreement between both approaches has been demonstrated.^{4,11,26,27} Note that in Ref. 4 the 3D model calculations are compared to experiment whereas the same results are obtained in Ref. 11 from the pseudo-one-dimensional (1D) analog. Similar agreement between both approaches is seen by comparing the calculated soft-mode frequencies of Refs. 26, 27, and 33. The current approach has, however, the advantage that it is parameter free as compared to its 3D analog and thus becomes highly transparent. In addition, the correctness of the numerical results can be readily tested analytically in the long-wavelength and the zone-boundary limits. The transition temperature is given by the condition $g_{T=T_c} = 0$. This limit corresponds to a long-wavelength displacive phase transition, but at finite momentum optic-acoustic mode-mode coupling sets in which induces dynamical finite-size clusters¹³ obeying different time and length scales than the soft mode. We conclude that, even in nominally purely displacive systems, order/disorder and displacive dynamics coexist. By using previously established values of the model parameters,¹¹ which were derived self-consistently, the transition temperatures T_c and T_s have been calculated (for the calculation of the structural instability as a function of ^{18}O content x the second-nearest-neighbor coupling has been changed to negative values,¹³ but kept the same for all x) and are shown in Figs. 1(a) and 1(b). It is important to note that no parameter has been changed and only the sublattice mass M_1 has been varied as described above.

In Fig. 1(a) the points where T_c is zero are those where quantum fluctuations suppress the instability. Note that in both Figs. 1(a) and 1(b) neither T_c nor T_s can be further enhanced by artificially enhancing M_1 ; they have reached their maximum values. This means that saturation of both T_c and T_s is achieved in the fully isotope replaced system. Also,

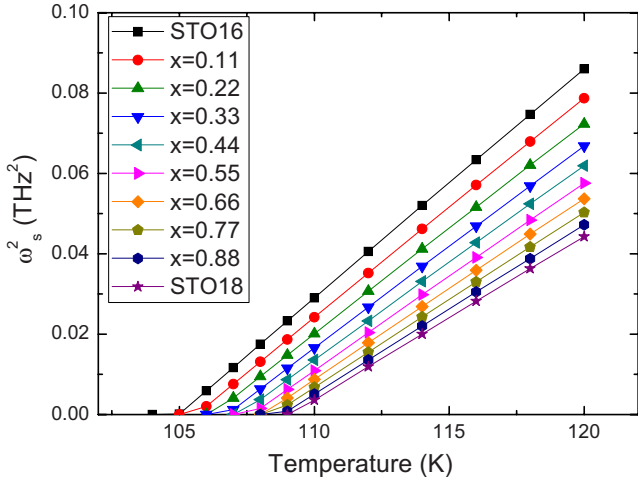


FIG. 2. (Color online) The squared structural soft-mode frequency ω_s^2 as a function of temperature for different values of x , as indicated in the figure, in $\text{STO}_{16_{1-x}}\text{STO}_{18_x}$.

the x dependence of each transition temperatures is very different: T_c shows a nonlinear dependence on x , whereas T_s increases almost linearly. In both case, however, the transition temperature does not follow a $1/\sqrt{M_1}$ dependence. The observation of the linear dependence of T_s on x is a consequence of the fact that, at elevated temperatures, the polarizability coordinate $\langle w^2 \rangle_T$ obeys a different power-law dependence on temperature than in the low-temperature regime, consistent with results obtained in Ref. 29. Similarly the two modes which drive the two phase transitions have a very different temperature dependence in the vicinity of the respective transition temperatures. The squared zone-boundary mode frequency ω_s^2 is shown in Fig. 2 as a function of x .

For all x a linear temperature dependence is observed where only the gradient decreases with increasing x . Such a behavior is typical for mean-field type phase transitions in spite of the fact that this transition is driven by polarizability effects. This behavior is in strong contrast to the low-

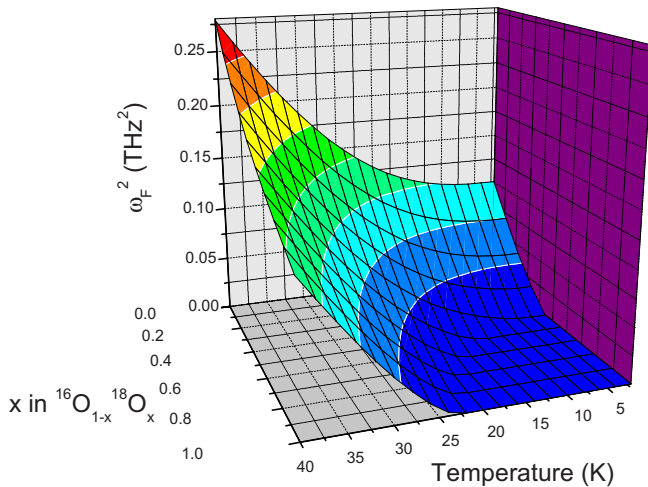


FIG. 3. (Color online) The squared ferroelectric soft-mode frequency ω_F^2 as a function of temperature and x , in $\text{STO}_{16_{1-x}}\text{STO}_{18_x}$.

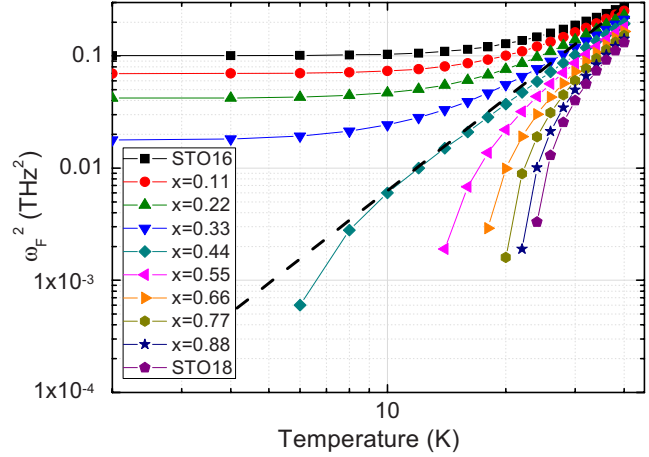


FIG. 4. (Color online) Double logarithmic plot of the squared soft-mode frequency ω_F^2 , as a function of temperature for different values of x indicated in the figure, in $\text{STO}_{16_{1-x}}\text{STO}_{18_x}$.

temperature dependence of the ferroelectric mode shown in Fig. 3.

First, we note that the x dependent modes are not shifted in parallel with increasing x . Second, for all values of x , ω_F^2 is nonlinearly dependent on temperature. Third, a distinctly different temperature dependence is observed for those value of x where a real instability takes place, as compared to the quantum paraelectric systems. This can be more clearly visualized by showing the same data as in Fig. 3 on a logarithmic scale (Fig. 4).

For values of x slightly larger than 0.35, a linear T^2 dependence is obeyed which indicates the dimensionality crossover.^{23,29} Logarithmic corrections set in with approaching T_c in accordance with renormalization-group predictions.²³ The onset of the linear T^2 dependence shifts to higher values of T with increasing x , i.e., increasing T_c . Thus the dimensionality crossover smoothly vanishes when T_c increases. For those compounds where quantum fluctuations

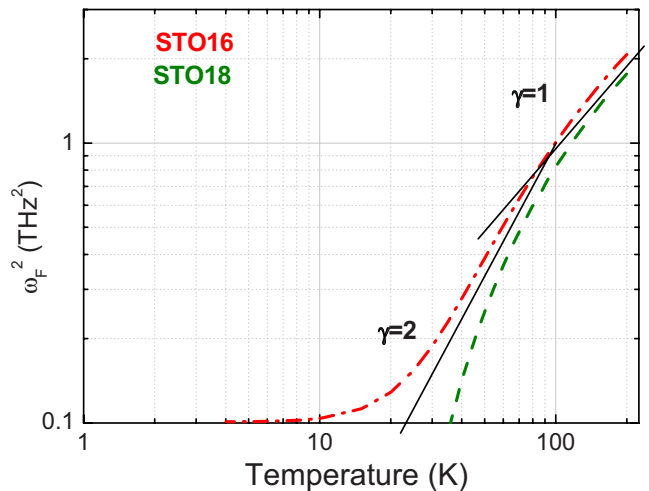


FIG. 5. (Color online) Double logarithmic plot of the squared soft-mode frequency ω_F^2 , as a function of temperature in STO_{16} (dash-dotted line) and STO_{18} (dashed line). The full lines indicate the classical and quantum regimes with critical exponent $\gamma=1,2$.

suppress the phase transition, a dimensionality crossover regime is again observed for x slightly less than $x=0.35$, where $\omega_F^2 \propto T^2$ throughout a broad temperature regime. This regime diminishes with decreasing x and is almost lost for STO16, where the onset temperature is beyond the temperature scale shown in Fig. 4. However, if increased temperatures are considered, the $\omega_F^2 \propto T^2$ regime recovers at higher temperatures and the crossover from $d=4$ to $d=3$ can be clearly observed (Fig. 5). For comparison, the results for STO18 are also included in the same Fig. 5. The black dashed line in Fig. 4 indicates the crossover from the ferroelectric regime to the quantum paraelectric one. Note that this line is the T^2 limit. The transition between both regimes is not continuous but of first order since the limit $T_c=0$ is never reached: either T_c remains finite or quantum fluctuations render temperature ineffective.

To summarize, we have systematically investigated the isotope dependence of the ferroelectric and structural phase transitions in $\text{STO}16_{1-x}\text{STO}18_x$ as a function of x . These

transitions show very different x dependences of their respective phase-transition temperatures. While the structural instability varies almost linearly with x , the ferroelectric instability is observed up to $x=0.35$ with a finite T_c . For $x < 0.35$ the transition is suppressed by quantum fluctuations. The dependence of T_c on x for $x > 0.35$ is nonlinear, as observed experimentally.¹⁰ The transition between the quantum fluctuation dominated and ferroelectric regimes is discontinuous, i.e., there is no evidence for a quantum critical point where $T_c=0$. The results are consistent with previous theoretical and experimental data,^{21–23,29} but extend these data since the crossover regime has been shown to be abrupt and the connection to the structural instability is provided with specific predictions for a x dependence of T_s . Since the polarizability model has been shown to yield extremely good agreement with experimental data,^{4,11,26,27,33} we consider the results to be of general validity and independent of the specific investigated compound.

¹G. Shirane and Y. Yamada, Phys. Rev. **177**, 858 (1969).

²K. A. Müller, W. Berlinger, and J. C. Slonczweski, Phys. Rev. Lett. **25**, 734 (1970).

³W. Cochran, Adv. Phys. **9**, 387 (1960); R. A. Cowley, Phys. Rev. **134**, A981 (1964); J. M. Worlock and P. A. Fleury, Phys. Rev. Lett. **19**, 1176 (1967).

⁴K. A. Müller and H. Burkard, Phys. Rev. B **19**, 3593 (1979).

⁵U. T. Höchli, K. Knorr, and A. Loidl, Adv. Phys. **39**, 405 (1990).

⁶I. S. Kim, M. Itoh, and T. J. Nakamura, J. Solid State Chem. **101**, 77 (1992).

⁷J. G. Bednorz and K. A. Müller, Phys. Rev. Lett. **52**, 2289 (1984).

⁸M. Itoh, R. Wang, Y. Inaguma, T. Yamaguchi, Y.-J. Shan, and T. Nakamura, Phys. Rev. Lett. **82**, 3540 (1999).

⁹For a recent critical review on Raman-scattering experiments, see T. Shigenari and K. Abe, Ferroelectrics (to be published).

¹⁰M. Takesada, M. Itoh, and T. Yagi, Phys. Rev. Lett. **96**, 227602 (2006).

¹¹A. Bussmann-Holder, H. Büttner, and A. R. Bishop, J. Phys.: Condens. Matter **12**, L115 (2000).

¹²R. Blinc, B. Zalar, V. V. Laguta, and M. Itoh, Phys. Rev. Lett. **94**, 147601 (2005).

¹³A. Bussmann-Holder, H. Büttner, and A. R. Bishop, Phys. Rev. Lett. **99**, 167603 (2007); A. Bussmann-Holder and A. R. Bishop, Europhys. Lett. **76**, 945 (2006).

¹⁴A. D. Bruce, K. A. Müller, and W. Berlinger, Phys. Rev. Lett. **42**, 185 (1979).

¹⁵T. Riste, E. Samuelson, K. Otnes, and J. Feder, Solid State Commun. **9**, 1455 (1971).

¹⁶S. M. Shapiro, J. D. Axe, G. Shirane, and T. Riste, Phys. Rev. B **6**, 4332 (1972).

¹⁷J. B. Hastings, S. M. Shapiro, and B. C. Frazer, Phys. Rev. Lett. **40**, 237 (1978).

¹⁸B. J. Halperin and C. M. Varma, Phys. Rev. B **14**, 4030 (1976).

¹⁹M. Holt, M. Sutton, P. Zschack, H. Hong, and T.-C. Chiang, Phys. Rev. Lett. **98**, 065501 (2007).

²⁰S. Ravy, D. Le Bolloc'h, R. Currat, A. Fluerasu, C. Mocuta, and B. Dkhil, Phys. Rev. Lett. **98**, 105501 (2007).

²¹R. Oppermann and H. Thomas, Z. Phys. B **22**, 387 (1975).

²²T. Schneider, H. Beck, and E. Stoll, Phys. Rev. B **13**, 1123 (1976).

²³D. Schmeltzer, Phys. Rev. B **28**, 459 (1983).

²⁴S. A. Prosandeev, W. Kleemann, B. Westwanski, and J. Dec, Phys. Rev. B **60**, 14489 (1999).

²⁵J. H. Barrett, Phys. Rev. **86**, 118 (1952).

²⁶R. Migoni, H. Bilz, and D. Bäuerle, Phys. Rev. Lett. **37**, 1155 (1976).

²⁷H. Bilz, G. Benedek, and A. Bussmann-Holder, Phys. Rev. B **35**, 4840 (1987).

²⁸A. N. Rubtsov and T. Janssen, Phys. Rev. B **63**, 172101 (2001).

²⁹D. Rytz, U. T. Höchli, and H. Bilz, Phys. Rev. B **22**, 359 (1980).

³⁰A. Chandra, R. Ranjan, D. P. Singh, N. Khare, and D. Pnaey, J. Phys.: Condens. Matter **18**, 2977 (2006).

³¹H. P. Soon and J. Wang, J. Appl. Phys. **100**, 124101 (2006).

³²A. Bussmann-Holder and H. Büttner, J. Phys.: Condens. Matter **14**, 7973 (2002).

³³A. Bussmann-Holder, H. Bilz, and G. Benedek, Phys. Rev. B **39**, 9214 (1989).